https://doi.org/10.5194/acp-2021-959
Preprint. Discussion started: 23 December 2021


Atmospheric Chemistry and Physics Discussions

# Measurement report: Ambient volatile organic compounds (VOCs) pollution at urban Beijing: characteristics, sources, and implications for pollution control

Lulu Cui[1], Di Wu[1], Shuxiao Wang[1,2*], Qingcheng Xu[1], Ruolan Hu[1], Jiming Hao[1, 2]

[1] *State Key Joint Laboratory of Environment Simulation and Pollution Control, School of Environment, Tsinghua University, Beijing 100084, China*

[2] *State Environmental Protection Key Laboratory of Sources and Control of Air Pollution Complex, Beijing 100084, China*

* Corresponding author. E-mail address: shxwang@tsinghua.edu.cn

## Abstract

The increasing ozone ($O_3$) pollution and high fraction of secondary organic aerosols (SOA) in fine particle mass highlighted the importance of volatile organic compounds (VOCs) in air pollution control. In this work, a campaign of comprehensive field observations was conducted at an urban site in Beijing, from December 2018 to November 2019, to identify the composition, sources, and secondary transformation potential of VOCs. The total mixing ratio of the 95 quantified VOCs (TVOC) observed in this study ranged from 5.5–118.7 ppbv with the mean value of 34.9 ppbv, and the contemporaneous mixing ratios of TVOC was significantly lower than those observed in 2014 and 2016, confirming the effectiveness of VOCs emission control measures in Beijing in recent years. Alkanes, OVOCs and halocarbons were the dominant chemical groups, accounting for 75-81% of the TVOCs across the sampling months. High and low-$O_3$/$PM_{2.5}$ months as well as several $O_3$/$PM_{2.5}$ polluted days were identified during the sampling period. By deweathered calculation, we found that high $O_3$/$PM_{2.5}$ levels were due to both enhanced precursor emission levels and meteorological conditions favorable to $O_3$ and $PM_{2.5}$ production. The molar ratios of VOCs to $NO_X$ indicated that $O_3$ formation was limited by VOCs during the whole sampling period. Diesel exhaust and industrial emission were identified as the major VOCs

https://doi.org/10.5194/acp-2021-959
Preprint. Discussion started: 23 December 2021


sources on both $O_3$-polluted and $PM_{2.5}$-polluted days based on positive matrix factorization (PMF) analysis, accounting for 46% and 53%, respectively. Moreover, higher proportion of oil/gas evaporation was observed on $O_3$-polluted days (18%) than that on $O_3$-clean days (13%), and higher proportion of coal/biomass combustion was observed on $PM_{2.5}$-polluted days (18%) than that on $PM_{2.5}$-clean days (13%). On the base of $O_3$ formation impact, VOCs from fuel evaporation and diesel exhaust particularly toluene, xylenes, trans-2-butene, acrolein, methyl methacrylate, vinyl acetate, 1-butene and 1-hexene were the main contributors, illustrating the necessity of conducting emission controls on these pollution sources and species for alleviating $O_3$ pollution. Instead, VOCs from diesel exhaust and coal/biomass combustion were found to be the dominant contributors for secondary organic aerosol formation potential (SOAFP), particularly the VOC species of toluene, 1-hexene, xylenes, ethylbenzene and styrene, and top priority should be given to these for the alleviation of haze pollution. The positive matrix factorization (PSCF) analysis showed that $O_3$ and $PM_{2.5}$ pollution was mainly affected by local emissions. This study provides insights for government to formulate effective VOCs control measures for air pollution in Beijing.

**Key words:** VOCs, OFP, SOAFP, Source appointment

https://doi.org/10.5194/acp-2021-959
Preprint. Discussion started: 23 December 2021




## 1. Introduction

The ozone ($O_3$) and fine particulate matter ($PM_{2.5}$) pollution has restricted improvements in air quality in China. Observation data from the Chinese Ministry of Environment and Ecolgy (MEE) network has witnessed an upward trend for $O_3$ across the country over the period 2013-2019 (Fu et al., 2019; Li et al., 2017; Li et al., 2020; Shen et al., 2019; Fan et al., 2020). Besides, haze pollution occurred in urban sites were commonly characterized by high fractions of secondary organic aerosols (SOA) in fine particles (Guo et al., 2014; Huang et al., 2014). Volatile organic compounds (VOCs) are key precursors for the formation of $O_3$ via multiphase reactions (Odum et al., 1997; Atkinson, 2000; Sato et al., 2010; Huang et al., 2014). In highly polluted urban regions, the $O_3$ formation was generally VOCs-limited, and it is suggested that VOCs emission control is necessary for effective alleviation of photochemical smog (Liu et al., 2020a,b; Shao et al., 2009; Wang et al., 2020; Xing et al., 2011). Besides, the VOCs compounds including aromatics and biogenic species have significant impact on SOA formation which play an important role in haze formation (Hallquist et al., 2009; Huang et al., 2014). VOCs emission abatement is therefore imperative for improving air quality in China.

VOCs in ambient air can be emitted by a variety of sources including both anthropogenic and biogenic sources. While biogenic emissions are more than 10 times that of anthropogenic emissions globally (Roger and Janet, 2003), anthropogenic emissions play the dominant role in urban and surrounding areas (Warneke et al., 2007; Ahmad et al., 2017; Wu and Xie, 2018). The VOC observations in China showed distinct differences in anthropogenic sources among different regions. For example, solvent use and vehicle exhaust are primary VOCs sources in urban Shanghai and urban Guangzhou, while the primary sources of VOCs in Wuhan, Zhengzhou and Beijing cities are combustion and vehicle exhaust (Han et al., 2020; Shen et al., 2020; Liu et al., 2020a; Li et al., 2019a). Apart from the diversity of emission sources, different VOCs species exhibited different propensities to

https://doi.org/10.5194/acp-2021-959
Preprint. Discussion started: 23 December 2021



form $O_3$ and SOA. Observation-based studies commonly applied the $O_3$ formation potential (OFP) and SOA formation potential (SOAFP) scales to quantify the relative effects of specific VOCs and sources on $O_3$ and SOA formation and to aid in the development of efficient control strategies (Carter and Atkinson, 1989; Chang and Rudy, 1990; Han et al., 2020; Zhang et al., 2017a). Although there have been many studies on ambient VOCs in various locations (e.g., urban, rural, and industrial areas), most of these measurements were confined to short periods (a few days or a certain season), and the understanding of temporal variations of concentrations, sources as well as the influence of photochemical reactions of VOCs on annual scale was still limited. Besides, most of the available reports on VOCs analysis based on online analytical techniques include mainly non-methane hydrocarbon compounds, and thus the characteristics of VOCs as well as their relationships with $PM_{2.5}$ and $O_3$ cannot be fully revealed since OVOC also participate actively in chemical reactions related to secondary formation (Li et al., 2019a; Zhao et al., 2020; Yang et al., 2018; Sinha and Sinha., 2019). Therefore, the long-term and comprehensive monitoring of VOCs are desired.

As the capital and one of the largest megacities in China, Beijing has been suffering from severe $O_3$ pollution due to rapid economic development and increases in precursor emissions (Wang et al., 2014; Wang et al, 2017; Li et al., 2019d; Zhao et al., 2020). According to the Report on the State of the Ecology and Environment in Beijing, the average 90th percentile $O_3$ daily maximum 8 h concentration in Beijing exceeded the national standards, reaching 193, 192, and 191 μg/m$^3$ in 2017, 2018, and 2019, respectively. In addition, the number of motor vehicles in Beijing reached 6.365 million at of the end of 2019 (http:// beijing.gov.cn), making Beijing the top city in China in terms of number of motor vehicles. The existing field measurements in Beijing were mostly conducted before 2016, and the observation in most recent years is quite limited (Li et al., 2015; Li et al., 2019c; Liu et al., 2020a; Yang et al., 2018). In this work, a campaign of comprehensive field observations was conducted

https://doi.org/10.5194/acp-2021-959
Preprint. Discussion started: 23 December 2021




at an urban site in Beijing during December 2018 and November 2019 for the analysis of VOCs. Several $O_3$ and $PM_{2.5}$ pollution events were captured during the sampling period. The characteristics and the contribution of specific species and sources of VOCs on $O_3$ and SOA formation, with a focus on photochemical and haze pollution periods, were analyzed in detail. The results and implications from this study can provide useful guidance for policymakers to alleviate ozone and haze pollution in Beijing.

# 2. Methodology

## 2.1 Field measurement

The sampling site is at the roof of a three-floor building on the campus of Tsinghua University (40.00°N, 116.33°E), northwest of Beijing urban area (Fig. S1). The altitude of the sampling site is 57 m. This sampling site is surrounded by school and there are no large emission sources nearby, therefore it can represent the urban air quality in Beijing. Details of the site description is found in Xu et al., (2019).

The air samples were collected using 6 L summa canisters (Entech, USA) with a stable rate of 4.26 ml/min. The samples were pre-processed to remove $N_2$, $O_2$, $CO_2$, CO and $H_2O$ in the samples and to further concentrate the samples in volume by the cryogenic pre-concentrator (Model 7100, Entech Instruments Inc., USA). Pressure gage was used to test if the canister has air leakage exist before sampling every time, and blanks were prepared using cleaned canisters to fill with high purity nitrogen. The cryotraps of precooling system was baked before analyses each day and between every samples. The VOCs in air samples were analyzed by a gas chromatography system (Agilent Tech., 7890/5975, USA). The column temperature was controlled by an initial temperature of -40 °C. The programmed temperature was used with helium as carrier gas, and the flow rate was set at 1.5 ml $min^{-1}$. The initial temperature was set at 90 °C, and then switched to 220 °C. The standard substance (SPECTRA GASES Inc., USA) mentioned for Photochemical Assessment Monitoring Stations (PAMS) and US EPA TO-15

https://doi.org/10.5194/acp-2021-959
Preprint. Discussion started: 23 December 2021


standard was used to construct the calibration curves for the 95 target VOCs, including 25 alkanes, 8 alkenes, 16 aromatics, 34 halocarbons and 12 OVOC. Quality assurance and quality control, including method detection limit (MDL) of each compound, laboratory and field blanks, retention time, accuracy and duplicate measurements of samples were performed according to USEPA Compendium Method TO-15 (USEPA 1999). The correlated coefficient of the calibration curves for all the compounds was > 0.95. The relative standard deviation for all of compounds of triplicates were 0.5%-6.0%

During the sampling periods, the measurements of $PM_{2.5}$, gaseous pollutants ($NO_X$ and $O_3$), and meteorological variables (such as temperature, relative humidity, wind speed, and wind direction) were conducted simultaneously. $NO_X$ and $O_3$ were analyzed using the Ozone Analyzer (Thermo Fisher Scientific USA, 49I) and NO–$NO_2$-$NO_X$ Analyzer (Thermo Fisher Scientific USA, 17I), respectively. The mass concentration of $PM_{2.5}$ was measured using an oscillating balance analyzer (TH-2000Z, China) (Wang et al., 2014). Meteorological including wind speed (WS), wind direction (WD), relative humidity (RH), air pressure, temperature, air pressure, and precipitation were measured by an automatic weather monitoring system. The planetary boundary height was obtained from the European Centre for Medium-Range Weather Forecasts (https://www.ecmwf.int/en/forestcasts/datasets/browse-reanalysis -datasets).

## 2.2 Ozone formation potential (OFP) and secondary formation potential (SOAFP) calculation

The formation potential of $O_3$ and SOA was used to characterize the relative importance of VOCs species and sources in secondary formation, which were estimated using Eqs. (1) and (2).

$$OFP = \sum_{i}^{n} MIR_i \times [VOC(ppb)]_i \quad (1)$$

$$SOAFP = \sum_{i}^{n} Y_i \times [VOC(ppb)]_i \quad (2)$$

https://doi.org/10.5194/acp-2021-959
Preprint. Discussion started: 23 December 2021


where $n$ represents the number of VOCs, [VOC]$i$ represents the $i$th VOC species concentration, MIR$i$ is the maximum incremental reactivity for the $i$th VOC species, and $Yi$ is the SOA yield of $VOC_i$ (McDonald et al., 2018). The MIR for each VOC species were taken from the updated Carter research results (http://www.engr.ucr.edu/~carter/reactdat.htm, last access: 24 February 2021). For species lacking yield curves, the fractional aerosol coefficient (FAC) values proposed by Grosjean and Seinfeld (1989) were used.

### 2.3 Deweathered model

In this work, a random forest (RF) model was used to assess the meteorology-associated variations and quantify the impacts of precursor emissions to $O_3$ and $PM_{2.5}$ levels. The meteorological predictors in the RF model include wind speed (*WS*), wind direction (*WD*), air temperature (*T*), relative humidity (*RH*), precipitation (*Prec*), air pressure (*P*), time predictors (year, day of year (*DOY*), hour) and planetary boundary layer height (*BLH*). These meteorological parameters have been reported to be strongly associated with $PM_{2.5}$ and $O_3$ concentrations in various regions in China (Chen et al., 2020; Feng et al., 2020) and contributed significantly in previous $PM_{2.5}$ and $O_3$ prediction models (She et al., 2020; Li et al., 2020). The original dataset was randomly classified into a training dataset (90 % of input dataset) for developing the RF model, and the remaining one was treated as the test dataset. After the building of the RF model, the deweathered technique was applied to predict the air pollutant level at a specific time point. The differences in original pollutant concentrations and deweathered pollutant concentrations were regarded as the concentrations contributed by meteorology. Statistical indicators including $R^2$, RMSE, and MAE values were regarded as the major criteria to evaluate the modeling performance.

### 2.4 Positive matrix factorization (PMF)

In this study, the US EPA PMF 5.0 software was used for VOCs source apportionment (Abeleira et al., 2017; Li et al., 2019a; Xue et al., 2017). The detailed description of the PMF model is found elsewhere (Ling et al., 2011;

https://doi.org/10.5194/acp-2021-959
Preprint. Discussion started: 23 December 2021




Yuan et al., 2009). PMF uses both concentration and user-provided uncertainty associated with the data to weight individual points. Species with high percentages of missing values (> 40 %) and with signal-to-noise ratio of below 2 were excluded. Based on this, 53 VOC species including source tracers (e.g., chloromethane, trichloroethylene, tetrachloroethylene and MTBE) and $SO_2$ were chosen for the source apportionment analysis. Data values below the MDL were replaced by MDL/2, and the missing data were substituted with median concentrations. If the concentration is less than or equal to the MDL provided, the uncertainty is calculated using the equation of Unc = 5/6 × MDL; if the concentration is greater than the MDL provided, the uncertainty is calculated as Unc = [(error faction × mixing ratio)$^2$+ (MDL)$^2$]1/2.

### 2.5 Cluster and potential source contribution function (PSCF) analysis

The potential source contribution function (PSCF) model has been widely used to identify potential source regions of air pollutants (Hong et al., 2019; Liu et al., 2016b, 2019, 2020a; Zheng et al., 2018;). In this study, the 24 h backward trajectories (1 h intervals) of air masses arriving at the sampling site with a trajectory height of 1500 m were calculated using the MeteoInfoMap software. The study area covered by back trajectories was divided into 0.5°×0.5° grid cells. The pollution trajectory was defined as the trajectories corresponding to the total VOC (TVOC) concentration that exceeded the 75th percentile concentration of TVOC. PSCF value in the *ij* th grid was defined as:

$$PSCF_{\mathrm{ij}} = \frac{m_{ij}}{n_{ij}} \tag{3}$$

where the $m_{ij}$ is the number of polluted trajectories through the grid; $n_{ij}$ is the all trajectories through the grid. The weight function $W_{ij}$ is applied to reveal the uncertainty of small values of nij (Polissar et al., 1999; Li et al., 2017):

https://doi.org/10.5194/acp-2021-959
Preprint. Discussion started: 23 December 2021




$$W_{ij} = \begin{cases} 1.00 & 80 < n_{ij} \\ 0.70 & 20 < n_{ij} \le 80 \\ 0.42 & 10 < n_{ij} \le 20 \\ 0.05 & n_{ij} \le 10 \end{cases} \quad (4)$$

# 3. Results and discussion

## 3.1 TVOC mixing ratios and chemical composition

The time series of meteorological parameters and concentrations of air pollutants during the measurement period are shown in Fig. 1. The ambient temperature ranged from -13.3°C to 38.7°C and the RH varied between 5% and 99% across the sampling months. Prevailing winds shifted between southwesterly and northeasterly with WS of 0–6.8 m $s^{-1}$. The mixing ratio of total VOCs (TVOC) ranged from 5.5–118.7 ppbv during the sampling period with relatively higher values during September and November (49.9-51.6 ppbv) while relatively lower values (22.2-27.5 ppbv) across the other months. Major VOC compositions were generally consistent during the whole measurement period. Alkanes, OVOCs and halocarbons were the dominant chemical groups, accounting for 75-81% of the TVOCs across the sampling months. In terms of individual species, acetone, dichloromethane, butane, toluene, methyl tert butyl ether (MTBE), *i*-pentane, propylene, hexane, 1,1- dichloroethane, benzene and 1-butene made up the largest contribution, accounting for 50.6 % of the TVOC on average during the whole measurement period.

The comparison of concentration and composition of chemical groups observed in this work and previous studies is shown in Fig. 2. Clearly, the concentrations of TVOCs and major VOC groups observed in this study were apparently lower than those in 2014 and 2016 in urban sites in Beijing (An et al., 2012; Liu et al., 2020a; Li et al., 2015b), indicating the effectiveness of control measures in most recent years on lowering VOCs emission. Besides, the composition of major chemical groups also showed remarkable changes, with decreased proportions

https://doi.org/10.5194/acp-2021-959
Preprint. Discussion started: 23 December 2021




of alkanes while increased fractions of halocarbons, aromatics and OVOCs, reflecting the changes in emission sources types in most recent years.

During the measurement period, nine $O_3$ pollution events (maximum daily 8-h average $O_3$ exceeding 160 μg $m^{-3}$) were observed, which occured during 17-22 April, 3-17 May, 18-29 June, 2-13 July, and 25-29 September of 2019. The months with $O_3$ pollution events were classified as high-$O_3$ months in this study, which were further classified into the clean and polluted days based on the measured concentrations. During the four high-$O_3$ months (i.e., April, May, June, July, and September), the WS on polluted days (1.31 ± 0.90 m $s^{-1}$) was slightly lower than that on clean days (1.47 ± 1.10 m $s^{-1}$), indicating that precursors were more conductive to be diluted on clean days. The variation trend of $O_3$ and temperature displayed the negative correlation, and the linear correlations between $O_3$ and temperature on polluted days ($R^2$ = 0.63) was stronger than that on clean days ($R^2$ = 0.35). The comparison of meteorological parameters and air pollutants concentrations on clean and polluted days is shown in Fig. 3. The mean TVOC concentration showed relatively higher values on pollution days (32.3 ppbv) than that on clean days (29.6 ppbv), which was mainly contributed by higher concentrations of MTBE, acrolein, trans-2-butene was higher on polluted days. MTBE is widely used as a fuel additive in motor gasoline (Liang et al., 2020), and trans-2-butene is the main component of oil/gas evaporation (Li et al., 2019a). Such result indicated enhanced contribution of traffic emissions on polluted days. Besides, the concentration of isoprene, which is primarily produced by vegetation through photosynthesis, increased significantly during the $O_3$ pollution day probably due to the stronger plant emission at elevated temperature (Guenther et al., 1993, 2012; Stavrakou et al., 2014). The ratio of *m/p*-xylene to ethylbenzene (X/E) measured can be used as an indicator of the photochemical aging of air masses because of their similar sources in urban environments and differences in atmospheric lifetimes (Carter., 2010; Miller et al., 2012; Wang et al., 2013). The mean X/E value on $O_3$ clean days (1.41) was higher

https://doi.org/10.5194/acp-2021-959
Preprint. Discussion started: 23 December 2021



than that on polluted days (1.17), indicating enhanced secondary transformation of VOCs to $O_3$ during the polluted periods.

The daily $PM_{2.5}$ concentrations ranged from 9-260 μg $m^{-3}$ with the mean value of 88.5 μg $m^{-3}$ during the measurement period. Fourteen $PM_{2.5}$ pollution events (daily average $PM_{2.5}$ exceeding 75 μg $m^{-3}$) were observed, which occured on 1-2 December and 5 December of 2018, 3 January, 12-13 January, 22-23 April, 29 April, 12 May, 15 May, 19 October, and 21-23 November of 2019. The months with $PM_{2.5}$ pollution events were classified as high-$PM_{2.5}$ months, which were also further classified into the clean and polluted days based on the measured concentrations. The WS on polluted days (1.05 ± 1.06 m $s^{-1}$) was lower than that on clean days (1.43 ± 1.06 m $s^{-1}$), indicating the weaker ability of winds for the dilution and diffusion of precursor on polluted days. Both the value of relative humidity (RH) and TVOCs increased significantly on polluted days, suggesting that the secondary transformation of VOCs was more conducive at high RH. The mean X/E value on $PM_{2.5}$ clean days (1.47) was slightly higher than that on polluted days (1.44), indicating enhanced secondary transformation of VOCs to $PM_{2.5}$ during the pollution periods.

## 3.2 The role of VOCs on secondary pollution

### 3.2.1 Estimating $O_3$ and $PM_{2.5}$ levels contributed by emissions

$O_3$ and secondary aerosols are primarily formed via photochemical reactions in the atmosphere, of which concentrations could be largely influenced by meteorological conditions (Chen et al., 2020; Feng et al., 2020; Zhai et al., 2019). In this work, the respective contributions of meteorology and emissions to $PM_{2.5}$ and $O_3$ variations were determined using the RF model as described in section 2.3. The coefficients of determination ($R^2$) for the RF model in predicting $PM_{2.5}$ and $O_3$ are 0.85 and 0.91, respectively (Shown in Fig. S2). The respective contributions of anthropogenic and meteorology to $O_3$ and $PM_{2.5}$ during each period is shown in Fig. 4. During

https://doi.org/10.5194/acp-2021-959
Preprint. Discussion started: 23 December 2021




the high-$O_3$ months, the meteorologically-driven $O_3$ on the polluted days (72.5 μg $m^{-3}$) was significantly higher than that on the clean days (35.3 μg $m^{-3}$). After removing the meteorological contribution, the residual emission-driven $O_3$ on polluted days (45.3 μg $m^{-3}$) and clean days (44.9 μg $m^{-3}$) of the high-$O_3$ months was almost identical and were significantly higher than that during the low-$O_3$ months (23.8 μg $m^{-3}$). The emission-driven $PM_{2.5}$ level was in the order of: polluted days of the high-$PM_{2.5}$ months (55 μg $m^{-3}$) > clean days of the high-$PM_{2.5}$ months (44 μg $m^{-3}$) > low-$PM_{2.5}$ months (29 μg $m^{-3}$). These results suggested that apart from meteorological factors, emissions also play a role in deteriorating $PM_{2.5}$ and $O_3$ pollution, and reducing anthropogenic emissions is essential for improving air quality.

The VOCs/$NO_X$ ratio has been widely used to distinguish whether the $O_3$ formation is VOC limited or $NO_X$ limited (Li et al., 2019a). Generally, VOC-sensitive regime occurs when VOCs/$NO_X$ ratios are below 10 while $NO_X$-sensitive regime occurs when VOCs/$NO_X$ ratios are higher than 20 (Hanna et al., 1996; Sillman, 1999). In this study, the values of VOCs/$NO_X$ (ppbv $ppbv^{-1}$) were all below 3 during both the $O_3$-polluted and low-$O_3$ months (Fig. S3), suggesting that the $O_3$ formation was sensitive to VOCs, and thus the reductions of the emissions of VOCs will be beneficial for $O_3$ alleviation.

### 3.2.2 Contribution of VOCs to OFP and SOAFP

As discussed in 3.1, $O_3$ formation was generally VOCs-sensitive during the measurement period. Quantifying the contribution of speciated VOCs species to $O_3$ is helpful for developing effective VOCs control measures and alleviating $O_3$ pollution. The averaged OFP on clean days of the high-$O_3$ months, polluted days of the high-$O_3$ months, and during the low-$O_3$ months were 201.4, 224.9 and 187.5 μg $m^{-3}$, respectively (Fig. 5). According to our observations, the higher OFP on $O_3$-polluted days of the high-$O_3$ months compared with that on clean days of the high-$O_3$ months was mainly contributed by higher levels of trans-2-butene, o-xylene and

https://doi.org/10.5194/acp-2021-959
Preprint. Discussion started: 23 December 2021




acrolein on polluted days, in line with that in Fig. 3. Alkenes, aromatics and OVOCs were the three contributing chemical groups to $O_3$ formation, accounting for 85.7%, 85.1% and 81.6% of the total OFP on clean days of the high-$O_3$ months, polluted days of the high-$O_3$ months, and during the low-$O_3$ months, respectively. In terms of the individual species, the top 10 highest contributors during the high-$O_3$ months were toluene (7.5% and 6.4% on $O_3$ clean and polluted days, respectively), trans-2-butene (7.5% and 9.6%), acrolein (5.7% and 10.8%), m/p-xylene (6.9% and 6.1%), o-xylene (5.8% and 6.6%), 1-butene (7.1% and 5.2%), 1-hexene (5.4% and 4.4%), vinyl acetate (5.7% and 4.2%), methyl methacrylate (4.8% and 5.5%), and 1-pentene (4.4% and 4.5%). During the low-$O_3$ months, the overall OFP was mainly contributed by toluene (10.8%), trans-2-butene (10.5%), 1-butene (7.3%), m/p-xylene (6.5%), 1-pentene (5.7%), 1-hexene (5.0%), methyl methacrylate (4.9%), o-xylene (4.9%), vinyl acetate (3.8%), and isopentane (2.3%), respectively.

As shown in Fig. 4, the ratio of VOCs/NOx was generally below 3 during the sampling period, indicating high $NO_X$ conditions. Based on the estimated yields of the VOCs shown in Table S1, the SOAFPs were calculated and compared in Fig. 5. The mean SOAFP on clean days of the high-$PM_{2.5}$ months, polluted days of the high-$PM_{2.5}$ months, and during the low-$PM_{2.5}$ months were 1.07, 1.28 and 0.89 μg $m^{-3}$, respectively. The higher SOAFP on $PM_{2.5}$-polluted days of the high-$PM_{2.5}$ months than that on clean days of the high-$PM_{2.5}$ months was mainly contributed by higher levels of 1,2,4-trimethylbenzene, n-undecanone, n-Nonane, 1,4-diethylbenzene, and 1,3-diethylbenzene on polluted days. Aromatics have the largest SOAFP, accounting for 75%, 74% and 70% of the total SOAFP on clean days of the high-$PM_{2.5}$ months, polluted days of the high-$PM_{2.5}$ months and during the low-$PM_{2.5}$ months, respectively. The 10 species responsible for most of the SOAFP were toluene (41% on polluted days of the high-$PM_{2.5}$ months, 40% on clean days of the high-$PM_{2.5}$ months, and 33% during the low-$PM_{2.5}$ months), 1-hexene (13.0%, 12.5%, and 15.2%), xylenes (11.6%, 14.1% and 14.8%), ethylbenzene (4.9%,

https://doi.org/10.5194/acp-2021-959
Preprint. Discussion started: 23 December 2021




5.3% and 6.0%), styrene (4.5%, 5.6% and 5.6%), 1-pentene (3.3%, 3.4% and 4.3%), methyl cyclopentane (2.1%, 2.7% and 3.6%), 1,2,3-trimethylbenzene (2.8%, 2.4% and 2.8%), m-ethyl toluene (1.7%, 1.4% and 1.7%) and p-ethyl toluene (1.7%, 1.4% and 1.7%), respectively.

### 3.3 Source apportionment of VOCs

The factor profiles given by PMF and the contribution of each source to ambient VOCs during each period is presented in Fig. 6 and Fig. 7, respectively. Six emission sources were identified: coal/biomass burning, solvent use, industrial sources, oil gas evaporation, gasoline vehicle emission, and diesel vehicle emission based on the corresponding markers for each source category. In general, diesel vehicle exhaust, gasoline vehicle exhaust and industrial emissions were the main VOCs sources during both $O_3$-polluted and $PM_{2.5}$-polluted months, with contributions of 62%, 62%, 52% and 66% on cleans days of the $O_3$-polluted months, polluted days of the $O_3$-polluted months, clean days of the $PM_{2.5}$-polluted months, and polluted days of the $PM_{2.5}$-polluted months, respectively. Diesel and gasoline vehicle exhaust exhibited obvious higher contributions while combustion and industrial sources showed lower contributions during the high-$O_3$ months than that during the low-$O_3$ months. The contributions of industrial emissions (22%) on $O_3$-polluted days were much higher than those on clean days (18%). Besides, the contribution of fuel evaporation (18%) also increased from 13% on $O_3$-clean days to 18% on $O_3$-pollution days. Figure 8 presents the relative contributions of individual VOC sources from PMF to OFP. On the base of $O_3$ formation impact, diesel and gasoline vehicle exhaust were major contributors as well, and the OFP of vehicle emissions on $O_3$-polluted days (93.9 μg $m^{-3}$) was higher than that on $O_3$-clean days (88.0 μg $m^{-3}$). Besides, fuel evaporation also showed higher OFP (35.5 μg $m^{-3}$) and served as an important contributor (18%) for $O_3$ formation on $O_3$-polluted days. Although industrial emissions act as an important source for VOCs concentrations on $O_3$-polluted days, the potential to form $O_3$ is limited, accounting for 11% of the total OFP. As

https://doi.org/10.5194/acp-2021-959
Preprint. Discussion started: 23 December 2021




shown in Fig., the industrial source was distinguished by high compositions of alkanes while relatively lower compositions of alkenes and aromatics, resulting in low $O_3$ formation potentials. Such results suggested that the fuel use and diesel vehicle exhaust should be controlled preferentially for $O_3$ mitigation.

The high-$PM_{2.5}$ months showed higher proportions of diesel vehicle emission (18%-24%) while lower proportions of industrial emission (12%-15%) compared with the low-$PM_{2.5}$ months (12% for diesel vehicle emission and 31% for industrial emission). The $PM_{2.5}$-polluted days were dominated by industrial emission (29%), diesel vehicle exhaust (24%), and combustion source (18%). Besides, the contribution of diesel vehicle exhaust and industrial sources on $PM_{2.5}$-polluted days (24% and 29%) were much higher than those on clean days (18% and 17%), and the contribution of combustion also increased to 18% during the transition of $PM_{2.5}$-clean days to 18%. On the base of $PM_{2.5}$ formation impact, diesel vehicle exhaust and combustion were two major contributors on $PM_{2.5}$-polluted days, and these two sources showed obvious higher SOAFP on $PM_{2.5}$-polluted days (0.30 and 0.32 μg $m^{-3}$, respectively) than that on $PM_{2.5}$-clean days (0.15 and 0.14 μg $m^{-3}$, respectively). Although industrial emissions act as an important source for VOCs concentrations on $PM_{2.5}$-polluted days, the potential to form $PM_{2.5}$ is limited, accounting for 16% of the total SOAFP. The above results suggested that diesel vehicle exhaust and combustion should be controlled preferentially for alleviating $PM_{2.5}$ pollution.

Based on the mass concentrations of individual species in each source, m/p-xylene, o-xylene, methyl methacrylate, vinyl acetate, 1-hexene, and acrolein in gasoline and diesel vehicular emissions; toluene, trans-2-butene, and 1-pentene in fuel evaporation and diesel vehicular emissions; acrolein in solvent, gasoline vehicular and diesel vehicular emissions were the dominant species contributing to photochemical $O_3$ formation (Fig. 9). Toluene, m/p-xylene, o-xylene, styrene, ethylbenzene, 1-pentene, 1,2,3-trimethylbenzene from combustion and diesel vehicular emissions; 1-hexene from diesel vehicular emission; and methyl cyclopentane from combustion,

https://doi.org/10.5194/acp-2021-959
Preprint. Discussion started: 23 December 2021



industrial and diesel vehicular emissions were the dominant contributors for SOA formation during the $PM_{2.5}$ pollution periods (Fig. 9).

### 3.4 Influence of source regions

Regional transport is an essential source for VOCs in addition to local emissions. The possible geographic origins of the VOC sources were explored using PSCF as shown in Fig. 10 and 11. Diversities of geographic origins were found for different periods. During the high-$O_3$ months, high PSCF values were found in Beijing and the junction of Hebei province while the PSCF showed high values in Inner Mongolia, northern Shanxi, Hebei, and Beijing during the clean months. The air mass backward trajectory cluster analysis indicated that the VOCs concentration was significantly affected by pollution transmission at the Shanxi Province and Hebei Province junction and local source emissions during the high-$O_3$ months. Note that the west short distance trajectories (cluster 1 in Fig. 10a) that passed over Shanxi and Hebei provinces exhibited relatively high VOCs concentrations and OFP, mainly contributed by aromatics. In addition, although the VOCs concentration of the trajectories from the south (cluster 3 in Fig. 10) was relatively small, the OFP in these pollution trajectories were the highest due to relatively higher proportion of aromatics. Therefore, in addition to local emissions, the transmission of highly polluting air masses from the western and southern Hebei should be paid attention for controlling emissions of reactive VOCs compounds. During the low-$O_3$ months, the VOCs concentration was mainly affected by the northwest trajectory that originate from Inner Mongolia and passed through the western Hebei, reflecting large-scale and long-distance transport of VOCs. Besides, the air masses from the southern region (cluster 1 in Fig. 10c), representing pollution transmission from Shanxi and Hebei provinces also have significant impact on VOCs concentration. Note that the VOCs concentration during the $O_3$-clean months were relatively higher compared with those during the polluted months. Fast-moving air masses from the northwest Inner Mongolia typically carry

https://doi.org/10.5194/acp-2021-959
Preprint. Discussion started: 23 December 2021




clean air masses (Zhang et al., 2017b). It is proposed that the higher VOCs concentration during the low-$O_3$ months was related to domestic coal/biomass burning in the northern regions during cold seasons. However, the OFP during the low-$O_3$ months were generally lower than those during pollution months, ascribing to lower contributions of OVOCs.

The VOCs concentration was mainly affected by local emissions on $PM_{2.5}$ polluted days according to the PSCF result. Besides, the air masses that originated from Inner and passed through western Hebei also played an important role in affecting the VOCs concentration as indicated by the relatively high VOCs concentration and SOAFP for this trajectory cluster. The south trajectories originating from the junction of Hebei province exhibited relatively low VOCs concentration. However, the SOAFP of this trajectory cluster was relatively high because of high proportion. Specifically, the proportion of southwest trajectories with high-density emissions to the total trajectories was higher on $PM_{2.5}$ pollution days (65.6%) than that on clean days (25.3%). During the low-$PM_{2.5}$ months, the VOCs concentration was mainly affected by the short distance northern (42.9%, cluster 2 in Fig. 11c) and western trajectories (29.8%, cluster 1 in Fig. 11c). Although the proportion of the southern trajectories (cluster 4 in Fig. 11c) to the total trajectories was relatively lower, both the VOCs concentration and the SOAFP of this trajectory cluster was the highest. Overall, the above results indicated that the transmission of highly polluting air masses from the junction of western and southern Hebei province should be paid attention for controlling emissions of reactive VOCs compounds and alleviating $PM_{2.5}$ pollution.

## 4. Conclusions

In this work, the field sampling campaign of VOCs was conducted during December 2018 and November 2019 to investigate the characteristics, sources and secondary transformation potential the role of VOCs at an urban site in Beijing. In total, 95 VOCs including 25 alkanes, 8 alkenes, 16 aromatics, 34 halocarbons and 12 OVOC

https://doi.org/10.5194/acp-2021-959
Preprint. Discussion started: 23 December 2021


were identified and quantified. The VOCs concentrations during the sampling period ranged from 5.5 to 118.7 ppbv with mean value of 34.9 ppbv. In terms of the composition, alkanes, OVOCs and halocarbons were the dominant chemical groups, accounting for 75-81% of the TVOCs across the sampling months. Nine $O_3$ pollution events and fourteen $PM_{2.5}$ pollution events were observed during the sampling period. By excluding the meteorological impact, the $O_3$ level driven by emissions during the $O_3$-polluted months were higher than that during the $O_3$-clean months, and similar pattern was found for $PM_{2.5}$. The molar ratio of VOCs to NO*x* indicated that $O_3$ formation was limited by VOCs during both the $O_3$-polluted and $O_3$-clean months, and thus reducing VOCs emission is essential for alleviation of $O_3$ pollution.

Six VOC sources were identified based on the PMF including coal/biomass combustion, solvent use, industrial sources, oil/gas evaporation, gasoline exhaust and diesel exhaust. By considering both the concentration and maximum incremental reactivity of individual VOC species for each source, fuel use and diesel exhaust sources particularly toluene, xylenes, trans-2-butene, acrolein, methyl methacrylate, vinyl acetate, 1-butene and 1-hexene were identified as the main contributors of $O_3$ formation during the $O_3$-polluted months, illustrating the necessity of conducting emission controls on these pollution sources and species for alleviating $O_3$ pollution. VOCs from diesel vehicles and combustion were found to be the dominant contributors for SOAFP, particularly the VOC species of toluene, 1-hexene, xylenes, ethylbenzene and styrene, and top priority should be given to these for the alleviation of haze pollution. The PSCF analysis showed that $O_3$ and $PM_{2.5}$ pollution was mainly affected by local emissions. Besides, the transmission of highly polluting air masses from the western and southern Hebei should also be paid attention for $O_3$ and $PM_{2.5}$ pollution control.

## Acknowledgements

This work was supported by the National Natural Science Foundation of China (21625701) and the Beijing Municipal Science and Technology Project (Z191100009119001 & Z181100005418018).

## Data availability

The meteorological data are available at http: //data.cma.cn/ (China Meteorological Administration). The website can be browsed in English http://data.cma.cn/en. The concentrations of air pollutants including $PM_{2.5}$, $O_3$ and $NO_X$ are available at https://air.cnemc.cn:18007/ (Ministry of Ecology and Environment the People's Republic of China). The website can be browsed in English http://english.mee.gov.cn/.

## References

Ahmad, W., Coeur, C., Tomas, A., Fagniez, T., Brubach, J. B., Cuisset, A., 2017. Infrared spectroscopy of secondary organic aerosol precursors and investigation of the hygroscopicity of SOA formed from the OH reaction with guaiacol and syringol. Appl. Opt. 56, E116, https://doi.org/10.1364/AO.56.00E116.

Abeleira, A., Pollack, I. B., Sive, B., Zhou, Y., Fischer, E. V., Farmer, D. K., 2017. Source characterization of volatile organic compounds in the Colorado Northern Front Range Metropolitan Area during spring and summer 2015, J. Geophys. Res.-Atmos., 122, 3595–3613, https://doi.org/10.1002/2016jd026227.

Atkinson, R., 2000. Atmospheric chemistry of VOCs and $NO_X$. Atmos. Environ. 34, 2063–2101, https://doi.org/10.1016/S1352-2310(99)00460-4.

An, J.L., Wang, Y.S., Wu, F.K., Zhu, B., 2012. Characterizations of volatile organic compounds during high ozone episodes in Beijing, China. Environ. Monit. Assess. 184, 1879e1889.

Carter, W.P.L. and Atkinson, R., 1989. Computer modeling study of incremental hydrocarbon reactivity. Environ. Sci. Technol. 23, 864–880, https://doi.org/10.1021/es00065a017.

https://doi.org/10.5194/acp-2021-959
Preprint. Discussion started: 23 December 2021




Carter, W.P.L., 2010. Development of the SAPRC-07 chemical mechanism, Atmos. Environ. 44, 5324–5335, https://doi.org/10.1016/j.atmosenv.2010.01.026.

Chang, T.Y. and Rudy, S.J., 1990. Ozone-forming potential of organic emissions from alternative-fueled vehicles, Atmos. Environ., 24, 2421–2430, https://doi.org/10.1016/0960-1686(90)90335-K.

Chen, L., Zhu, J., Liao, H., Yang, Y., Yue, X., 2020. Meteorological influences on $PM_{2.5}$ and $O_3$ trends and associated health burden since China's clean air actions, Sci. Total Environ. 744, 140837, https://doi.org/10.1016/j.scitotenv.2020.140837.

Fan, H., Zhao, C., Yang, Y., 2020. A Comprehensive Analysis of the Spatio-Temporal Variation of Urban Air Pollution in China During 2014–2018, Atmos. Environ., 220, 117066, https://doi.org/10.1016/j.atmosenv.2019.117066.

Feng, J., Liao, H., Li, Y., Zhang, Z., Tang, Y., 2020. Long-term trends and variations in haze-related weather conditions in north China during 1980–2018 based on emission-weighted stagnation intensity. Atmos. Environ. 240, 117830, https://doi.org/10.1016/j.atmosenv.2020.117830.

Fu, Y., Liao, H., Yang, Y., 2019. Interannual and Decadal Changes in Tropospheric Ozone in China and the Associated Chemistry Climate Interactions: A Review, Adv. Atmos. Sci. 36, 975–993.

Grosjean, D., and Seinfeld, J. H., 1989. Parameterization of the formation potential of secondary organic aerosols, Atmos. Environ., 23, 1733-1747, 10.1016/0004- 6981(89)90058-9.

Guenther, A.B., Zimmerman, P.R., Harley, P.C., Monson, R.K., Fall, R., 1993. Isoprene and monoterpene emission rate variability: Model evaluations and sensitivity analyses. J. Geophys. Res. Atmos. 98, 12609–12617, https://doi.org/10.1029/93JD00527.

https://doi.org/10.5194/acp-2021-959
Preprint. Discussion started: 23 December 2021




Guo, S., Hu, M., Zamora, M. L., Peng, J., Shang, D., Zheng, J., Du, Z., Wu, Z., Shao, M., Zeng, L., Molina, M. J., Zhang, R., 2014. Elucidating severe urban haze formation in China, P Natl. Acad. Sci. US, 111, 17373-17378.

Hallquist, M., Wenger, J.C., Baltensperger, U., Rudich, Y., Simpson, D., Claeys, M., et al., 2009. The formation, properties and impact of secondary organic aerosol: current and emerging issues. Atmos. Chem & Phys. 9 (14), 5155–5236.

Han, S., Zhao, Q., Zhang, R., Liu, Y., Li, C., Zhang, Y., Li, Y., Yin, S., Yan, Q., 2020. Emission characteristic and environmental impact of process-based VOCs from prebaked anode manufacturing industry in Zhengzhou, China. Atmos. Pollut. Res. 627 11, 67-77, 10.1016/j.apr.2019.09.016.

Hanna, S. R., Moore, G. E., Fernau, M., 1996. Evaluation of photochemical grid models (UAM-IV, UAM-V, and the ROM/UAMIV couple) using data from the Lake Michigan Ozone Study (LMOS). Atmos. Environ. 30, 3265–3279.

Hong, Z., Li, M., Wang, H., Xu, L., Hong, Y., Chen, J., Chen, J., Zhang, H., Zhang, Y., Wu, X., Hu, B., Li, M., 2019. Characteristics of atmospheric volatile organic compounds (VOCs) at a mountainous forest site and two urban sites in the southeast of China. Sci. Total. Environ. 657, 1491–1500, https://doi.org/10.1016/j.scitotenv.2018.12.132.

Huang, R.J., Zhang, Y., Bozzetti, C., Ho, K.F., Cao, J.J., Han, Y., Daellenbach, K. R., Slowik, J. G., Platt, S. M., Canonaco, F., Zotter, P., Wolf, R., Pieber, S. M., Bruns, E. A., Crippa, M., Ciarelli, G., Piazzalunga, A., Schwikowski, M., Abbaszade, G., Schnelle-Kreis, J., Zimmermann, R., An, Z., Szidat, S., Baltensperger, U., El Haddad, I., Prevot, A.S.H., 2014. High secondary aerosol contribution to particulate pollution during haze events in China, Nature, 514, 218-222, 10.1038/nature13774.

https://doi.org/10.5194/acp-2021-959
Preprint. Discussion started: 23 December 2021




Li, J., Xie, S.D., Zeng, L.M., Li, L.Y., Li, Y.Q., Wu, R.R., 2015. Characterization of ambient volatile organic compounds and their sources in Beijing, before, during, and after Asia-Pacific Economic Cooperation China 2014. Atmos. Chem. Phys.15, 7945–7959

Li, G., Bei, N., Cao, J., Wu, J., Long, X., Feng, T., Dai, W., Liu, S., Zhang, Q., Tie, X., 2017. Widespread and persistent ozone pollution in eastern China during the non-winter season of 2015: observations and source attributions, Atmos. Chem. Phys., 17, 2759–2774, https://doi.org/10.5194/acp-17-2759-2017.

Li, B., Ho, S.S.H., Gong, S., Ni, J., Li, H., Han, L., Yang, Y., Qi, Y., Zhao, D., 2019a. Characterization of VOCs and their related atmospheric processes in a central Chinese city during severe ozone pollution periods. Atmos. Chem & Phys. 19, 617-638.

Li, K., Jacob, D.J., Liao, H., Shen, L., Zhang, Q., Bates, K.H., 2019c. Anthropogenic Drivers of 2013−2017 Trends in Summer Surface Ozone in China. Proc. Natl. Acad. Sci. 116, 422−427.

Li, K., Li, J., Tong, S., Wang, W., Huang, R.-J., Ge, M., 2019d. Characteristics of wintertime VOCs in suburban and urban Beijing: concentrations, emission ratios, and festival effects. Atmos. Chem & Phys. 19, 8021-8036.

Li, K., Jacob, D.J., Shen, L., Lu, X., De Smedt, I., Liao, H., 2020. Increases in surface ozone pollution in China from 2013 to 2019: anthropogenic and meteorological influences. Atmos. Chem & Phys. 20, 11423-11433.

Liang, Y., Liu，X., Wu，F., Guo, Y., Xiao, H., 2020. The year-round variations of VOC mixing ratios and their sources in Kuytun City (northwestern China), near oilfields. Atmos. Pollut. Res. 11,9 DOI:10.1016/j.apr.2020.05.022.

Liu, B., Liang, D., Yang, J., Dai, Q., Bi, X., Feng, Y., Yuan, J., Xiao, Z., Zhang, Y., Xu, H., 2016a. Characterization and source apportionment of volatile organic compounds based on 1-year of observational data in Tianjin, China. Environ. Pollut. 218, 757–769, https://doi.org/10.1016/j.envpol.2016.07.072.

https://doi.org/10.5194/acp-2021-959
Preprint. Discussion started: 23 December 2021




Liu, B. S., Liang, D. N., Yang, J. M., Dai, Q. L., Bi, X. H., Feng, Y. C., Yuan, J., Xiao, Z. M., Zhang, Y. F., and Xu, H., 2019b. Characterization and source apportionment of volatile organic compounds based on 1-year of observational data in Tianjin, China. Environ. Pollut. 218, 757–769, https://doi.org/10.1016/j.envpol.2016.07.072.

Liu, Y., Wang, H., Jing, S., Gao, Y., Peng, Y., Lou, S., Cheng, T., Tao, S., Li, L., Li, Y., 2019. Characteristics and sources of volatile organic compounds (VOCs) in Shanghai during summer: Implications of regional transport. Atmospheric Environment 215, 116902.

Liu, Y.F., Song, M.D., Liu, X.G., Zhang, Y.P., Hui, L.R., Kong, L.W., Zhang, Y.Y., Zhang, C., Qu, Y., An, J.L., Ma, D.P., Tan, Q.W., Feng, M., 2020a. Characterization and sources of volatile organic compounds (VOCs) and their related changes during ozone pollution days in 2016 in Beijing, China. Environ Pollut. 257, 113599.

Liu, Y.M., Wang, T., 2020b. Worsening urban ozone pollution in China from 2013 to 2017–Part 2: The effects of emission changes and implications for multi-pollutant control. Atmos. Chem. Phys. 20, 6323–6337.

Liu, C., Shi, K., 2021. A review on methodology in O3-NOx-VOC sensitivity study. Environmental pollution, 118249.

Lu, X., Zhang, L., Wang, X., Gao, M., Li, K., Zhang, Y., Yue, X., Zhang, Y., 2020. Rapid increases in warm-season surface ozone and resulting health impact in China since 2013. Environ. Sci & Technol Lett. 7, 240-247.

McDonald, B.C., de Gouw, J.A., Gilman, J.B., Jathar, S.H., Akherati, A., Cappa, C.D., Jimenez, J.L., Lee-Taylor, J., Hayes, P.L., McKeen, S.A., Cui, Y.Y., Kim, S.W., Gentner, D.R., Isaacman-VanWertz, G., Goldstein, Allen H., Harley, R.A., Frost, G.J., Roberts, J. M., Ryerson, T.B., Trainer, M., 2018. Volatile chemical products emerging as largest petrochemical source of urban organic emissions, Science, 359, 760, https://doi.org/10.1126/science.aaq0524.

Miller, L., Xu, X., Grgicak-Mannion, A., Brook, J., Wheeler, A., 2012. Multi-season, multiyear concentrations and correlations amongst the BTEX group of VOCs in an urbanized industrial city. Atmos. Environ. 61, 305–315.

Odum, J.R., Jungkamp, T.P.W., Griffifin, R.J., Flagan, R.C., Seinfeld, J.H., 1997. The atmospheric aerosol-forming potential of whole gasoline vapor. Science. 276, 96–99.

Peng, J., Hu, M., Shang, D., Wu, Z., Du, Z., Tan, T., Wang, Y., Zhang, F., Zhang, R., 2021. Explosive secondary aerosol formation during severe haze in the North China Plain. Environ Sci & Technol. 55, 2189-2207.

Polissar, A.V., Hopke, P.K., Paatero, P., Kaufmann, Y.J., Hall, D.K., Bodhaine, B.A., Dutton, E.G., Harris, J.M., 1999. The aerosol at Barrow, Alaska: long-term trends and source locations. Atmos. Environ. 33, 2441–2458, https://doi.org/10.1016/S1352- 2310(98)00423-3, 1999.

Roger, A. and Janet, A., 2003. Atmospheric degradation of volatile organic compounds. Chem. Rev. 103, 4605, https://doi.org/10.1021/cr0206420.

Sato, K., Takami, A., Isozaki, T., Hikida, T., Shimono, A., Imamura, T., 2010. Mass spectrometric study of secondary organic aerosol formed from the photo-oxidation of aromatic hydrocarbons. Atmos. Environ. 44, 1080–1087, https://doi.org/10.1016/j.atmosenv.2009.12.013.

Shao, M., Zhang, Y., Zeng, L., Tang, X., Zhang, J., Zhong, L., Wang, B., 2009. Ground-level ozone in the Pearl River Delta and the roles of VOC and NOx in its production. J. Environ. Manage. 90, 512-518.

She, Q., Choi, M., Belle, J. H., Xiao, Q., Bi, J., Huang, K., Meng, X., Geng, G., Kim, J., He, K., Liu, M., Liu, Y., 2020. Satellite-based estimation of hourly PM2.5 levels during heavy winter pollution episodes in the Yangtze River Delta, China. Chemosphere. 239, 124678, https://doi.org/10.1016/j.chemosphere.2019.124678.

https://doi.org/10.5194/acp-2021-959
Preprint. Discussion started: 23 December 2021




Shen, L., Jacob, D. J., Liu, X., Huang, G., Li, K., Liao, H., Wang, T, 2019. An evaluation of the ability of the Ozone Monitoring Instrument (OMI) to observe boundary layer ozone pollution across China: application to 2005–2017 ozone trends. Atmos. Chem. Phys. 19, 6551–6560, https://doi.org/10.5194/acp-19-6551-2019.

Shen, L., Wang, Z., Cheng, H., Liang, S., Xiang, P., Hu, K., Yin, T., Yu, J., 2020. A Spatial-Temporal Resolved Validation of Source Apportionment by Measurements of Ambient VOCs in Central China, Int. J. Env. Res. Pub. He. 17, 791, https://doi.org/10.3390/ijerph17030791.

Sillman, S., 1999. The relation between ozone, NOx and hydrocarbons in urban and polluted rural environments, Atmos. Environ., 33, 1821–1845, 1999.

Sinha, B.P. and Sinha, V., 2019. Source apportionment of volatile organic compounds in the northwest Indo-Gangetic Plain using a positive matrix factorization model. Atmos. Chem. Phys. 19, 15467–15482.

Stavrakou, T., Müller, J.-F., Bauwens, M., De Smedt, I., Van Roozendael, M., Guenther, A., Wild, M., Xia, X., 2014. Isoprene emissions over Asia 1979–2012: impact of climate and land-use changes, Atmos. Chem. Phys., 14, 4587–4605, https://doi.org/10.5194/acp-14-4587-2014.

Sun, W., Wang, D., Yao, L., Fu, H., Fu, Q., Wang, H., Li, Q., Wang, L., Yang, X., Xian, A. (2019) Chemistry-triggered events of PM2. 5 explosive growth during late autumn and winter in Shanghai, China. Environmental pollution 254, 112864.

Wang, H.L., Chen, C.H., Wang, Q., Huang, C., Su, L.Y., Huang, H.Y., Lou, S.R., Zhou, M., Li, L., Qiao, L.P., Wang, Y.H., 2013. Chemical loss of volatile organic compounds and its impact on the source analysis through a two-year continuous measurement. Atmos. Environ. 80, 488–498.

https://doi.org/10.5194/acp-2021-959
Preprint. Discussion started: 23 December 2021


Wang, Y.S., Yao, L., Wang, L.L., Liu, Z.R., Ji, D.S., Tang, G. Q., Zhang, J.K., Sun, Y., Hu, B., Xin, J.Y., 2014. Mechanism for the formation of the January 2013 heavy haze pollution episode over central and eastern China. Sci. China Earth Sci. 57, 14–25, https://doi.org/10.1007/s11430-013-4773-4.

Wang, T., Xue, L., Brimblecombe, P., Lam, Y.F., Li, L., Zhang, L., 2017. Ozone Pollution in China: A Review of Concentrations, Meteorological Influences, Chemical Precursors, and Effects. Sci. Total Environ. 575, 1582−1596.

Wang, J., Yang, Y., Zhang, Y., Niu, T., Jiang, X., Wang, Y., Che, H., 2019. Influence of meteorological conditions on explosive increase in O3 concentration in troposphere. Sci.Total Environ. 652, 1228-1241.

Wang, M, L., Li, S.Y., Zhu, R.C., Zhang, R.Q., Zu, L., Wang, Y.J., Bao, X.F., 2020. On-road tailpipe emission characteristics and ozone formation potentials of VOCs from gasoline, diesel and liquefied petroleum gas fueled vehicles. Atmos. Environ. 223, 117294.

Warneke, C., McKeen, S. A., de Gouw, J. A., Goldan, P. D., Kuster, W. C., Holloway, J. S., Williams, E. J., Lerner, B. M., Parrish, D. D., Trainer, M., Fehsenfeld, F. C., Kato, S., Atlas, E. L., Baker, A., Blake, D. R., 2007. Determination of urban volatile organic compound emission ratios and comparison with an emissions database. J. Geophys. Res. 112, D10S47, https://doi.org/10.1029/2006jd007930.

Wu, R. and Xie, S., 2018. Spatial Distribution of Secondary Organic Aerosol Formation Potential in China Derived from Speciated Anthropogenic Volatile Organic Compound Emissions, Environ. Sci. Technol. 52, 8146–8156, https://doi.org/10.1021/acs.est.8b01269.

Xing, J., Wang, S. X., Jang, C., Zhu, Y., Hao, J. M., 2011. Nonlinear response of ozone to precursor emission changes in China: a modeling study using response surface methodology. Atmos. Chem. Phys. 11, 5027–5044, https://doi.org/10.5194/acp-11-5027-2011.

https://doi.org/10.5194/acp-2021-959
Preprint. Discussion started: 23 December 2021




Xu Q, Wang S, Jiang J., 2019. Nitrate dominates the chemical composition of PM2.5 during haze event in Beijing, China. Sci. Total. Environ. 689:1293-1303.

Xue, Y., Ho, S. S. H., Huang, Y., Li, B., Wang, L., Dai, W., Cao, J., Lee, S., 2017. Source apportionment of VOCs and their impacts on surface ozone in an industry city of Baoji, Northwestern China. Sci. Rep. 7, 9979, https://doi.org/10.1038/s41598-017-10631-4.

Xue, T., Zheng, Y., Geng, G., Xiao, Q., Meng, X., Wang, M., Li, X., Wu, N., Zhang, Q., Zhu, T., 2020a. Estimating Spatiotemporal Variation in Ambient Ozone Exposure during 2013–2017 Using a Data-Fusion Model. Environ Sci. Technol. 54, 14877-14888.

Xue, Y., Huang, Y., Ho, S.S.H., Chen, L., Wang, L., Lee, S., Cao, J., 2020b. Origin and transformation of ambient volatile organic compounds during a dust-to-haze episode in northwest China. Atmos. Chem. Phys. 20, 5425-5436.

Yang, W.Q., Zhang, Y.L., Wang, X.M., Li, S., Zhu, M., Yu, Q.Q., Li, G.H., Huang, Z.H., Zhang, H.N., Wu, Z.F., Song, W., Tan, J.H., Shao, M., 2018. Volatile organic compounds at a rural site in Beijing: influence of temporary emission control and wintertime heating. Atmos. Chem. Phys. 18, 12663–12682.

Yao, L., Wang, D., Fu, Q., Qiao, L., Wang, H., Li, L., Sun, W., Li, Q., Wang, L., Yang, X., 2019. The effects of firework regulation on air quality and public health during the Chinese Spring Festival from 2013 to 2017 in a Chinese megacity. Environ Int. 126, 96-106.

Zhai, S., Jacob, D.J., Wang, X., Shen, L., Li, K., Zhang, Y., Gui, K., Zhao, T., Liao, H., 2019. Fine particulate matter ($PM_{2.5}$) trends in China, 2013–2018: separating contributions from anthropogenic emissions and meteorology, Atmos. Chem. Phys. 19, 11031– 11041, https://doi.org/10.5194/acp-19-11031-2019.

https://doi.org/10.5194/acp-2021-959
Preprint. Discussion started: 23 December 2021




Zhang, X., Xue, Z., Li, H., Yan, L., Yang, Y., Wang, Y., Duan, J., Li, L., Chai, F., Cheng, M., Zhang, W., 2017a. Ambient volatile organic compounds pollution in China, J Environ. Sci., 55, 69-75, 10.1016/j.jes.2016.05.036.

Zhang, H., Li, H., Zhang, Q., Zhang, Y., Zhang, W., Wang, X., Bi, F., Chai, F., Gao, J., Meng, L., Yang, T., Chen, Y., Cheng, Q., Xia, F., 2017b. Atmospheric Volatile Organic Compounds in a Typical Urban Area of Beijing: Pollution Characterization, Health Risk Assessment and Source Apportionment. Atmosphere 8, 61.

Zhang, Y., Li, R., Fu, H., Zhou, D., Chen, J., 2018. Observation and analysis of atmospheric volatile organic compounds in a typical petrochemical area in Yangtze River Delta, China. J. Environ. Sci. 71, 233-248.

Zhao, D., Liu, G., Xin, J., Quan, J., Wang, Y., Wang, X., 2020. Haze pollution under a high atmospheric oxidization capacity in summer in Beijing: insights into formation mechanism of atmospheric physicochemical processes. Atmos. Chem. Phys. 20, 4575-4592.

Zhao, Q.Y., Bi, J., Liu, Q., Ling, Z.H., Shen, G.F., Chen, F., Qiao, Y.Z., Li, C.Y., Ma, Z.W., 2020. Sources of volatile organic compounds and policy implications for regional ozone pollution control in an urban location of Nanjing, East China. Atmos. Chem. Phys. 20, 3905–3919.

Zheng, H., Kong, S., Xing, X., Mao, Y., Hu, T., Ding, Y., Li, G., Liu, D., Li, S., Qi, S., 2018. Monitoring of volatile organic compounds (VOCs) from an oil and gas station in northwest China for 1 year. Atmos. Chem. Phys. 18, 4567-4595.

https://doi.org/10.5194/acp-2021-959
Preprint. Discussion started: 23 December 2021




## Figure captions

**Figure 1.** Time series of meteorological parameters and levels of air pollutants during the sampling period.

**Figure 2.** Comparison of the concentration and composition of major chemical groups observed in 2019 (this study), 2016 (Liu et al., 2020) and 2014 (Li et al., 2015).

**Figure 3.** Comparison of major meteorological parameters and air pollutants on clean and polluted days.

**Figure 4.** Statistic decomposition of meteorological and emission contribution to $O_3$ and $PM_{2.5}$ levels during different periods.

**Figure 5.** OFP and SOAFP by chemical groups during different periods.

**Figure 6.** Source profiles of VOCs identified using the PMF model and the relative contributions of the individual VOC species.

**Figure 7.** Contributions of each source to VOCs during different periods.

**Figure 8.** Contributions of each source to OFP and SOAFP during different periods.

**Figure 9.** OFP values of the dominant VOC species in the different source categories during the on polluted (a) and clean (b) days of the high-$O_3$ months, and SOAFP values on polluted (c) and clean (d) days of the high-$PM_{2.5}$ months.

**Figure 10.** Backward trajectory cluster analysis (24 h) and PSCF analysis during different periods: (a) polluted days of the high-$O_3$ months, (b) clean days of the high-$O_3$ months, (c) low-$O_3$ months.

**Figure 11.** Backward trajectory cluster analysis (24 h) and PSCF analysis during different periods: (a) polluted days of the high-$PM_{2.5}$ months, (b) clean days of the high- $PM_{2.5}$ months, (c) low- $PM_{2.5}$ months.

https://doi.org/10.5194/acp-2021-959
Preprint. Discussion started: 23 December 2021


Atmospheric Chemistry and Physics Discussions
Open Access

**Fig. 1.**

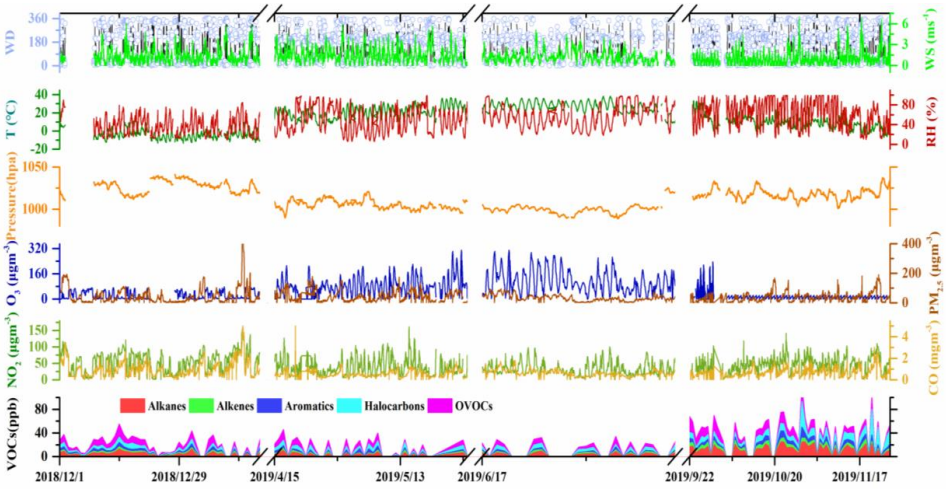

https://doi.org/10.5194/acp-2021-959
Preprint. Discussion started: 23 December 2021




**Figure 2.**

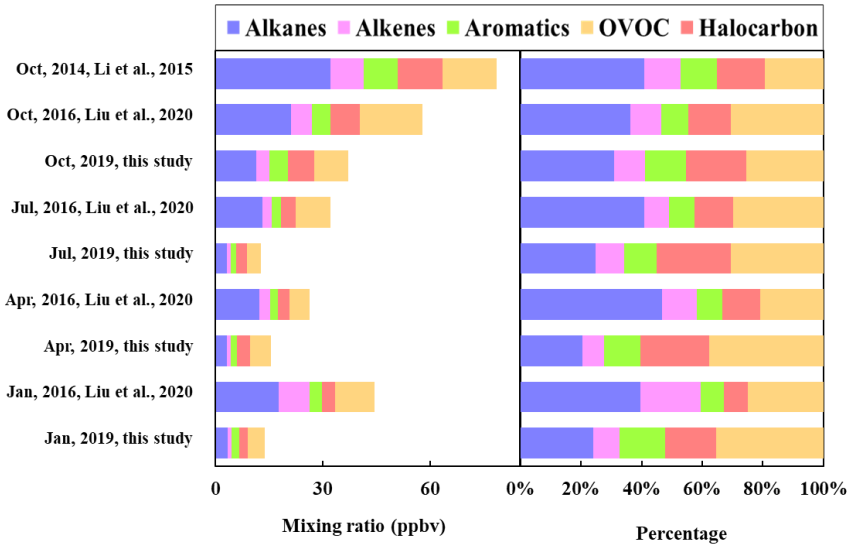

https://doi.org/10.5194/acp-2021-959
Preprint. Discussion started: 23 December 2021


Atmospheric Chemistry and Physics Discussions

**Fig. 3.**

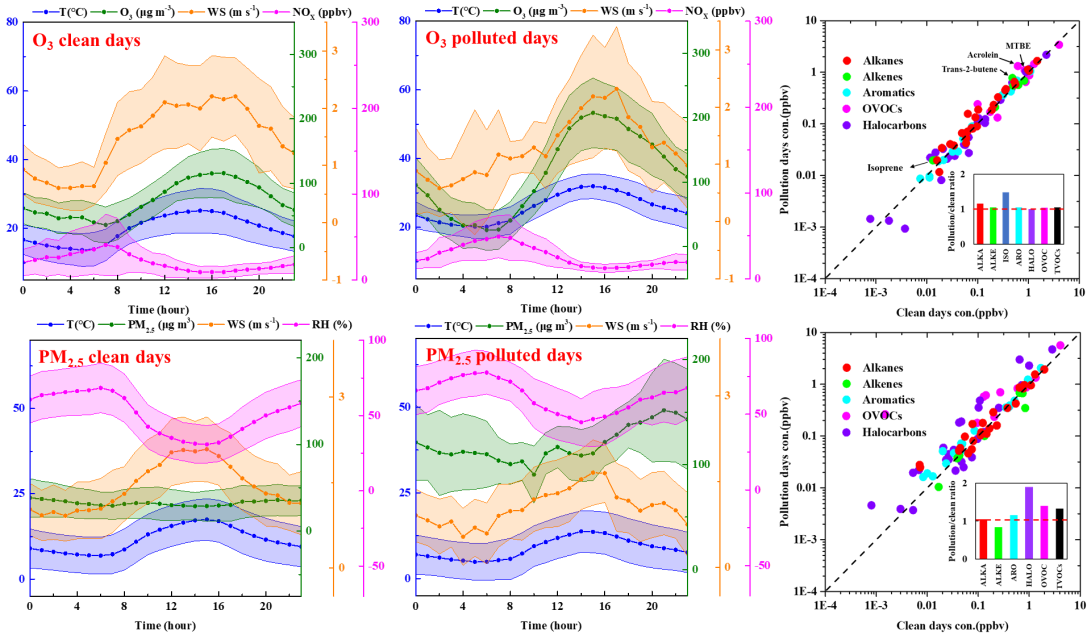

https://doi.org/10.5194/acp-2021-959
Preprint. Discussion started: 23 December 2021




**Fig. 4**

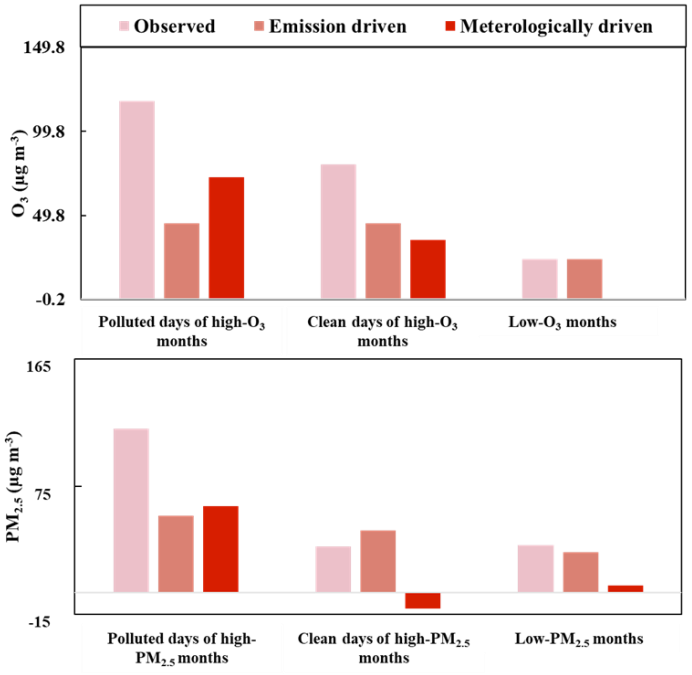

https://doi.org/10.5194/acp-2021-959
Preprint. Discussion started: 23 December 2021




**Fig. 5**

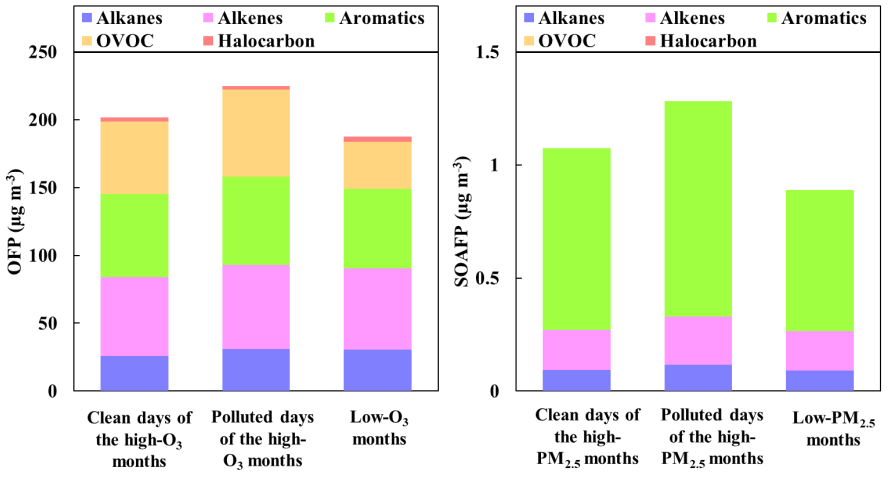

https://doi.org/10.5194/acp-2021-959
Preprint. Discussion started: 23 December 2021




**Fig. 6.**

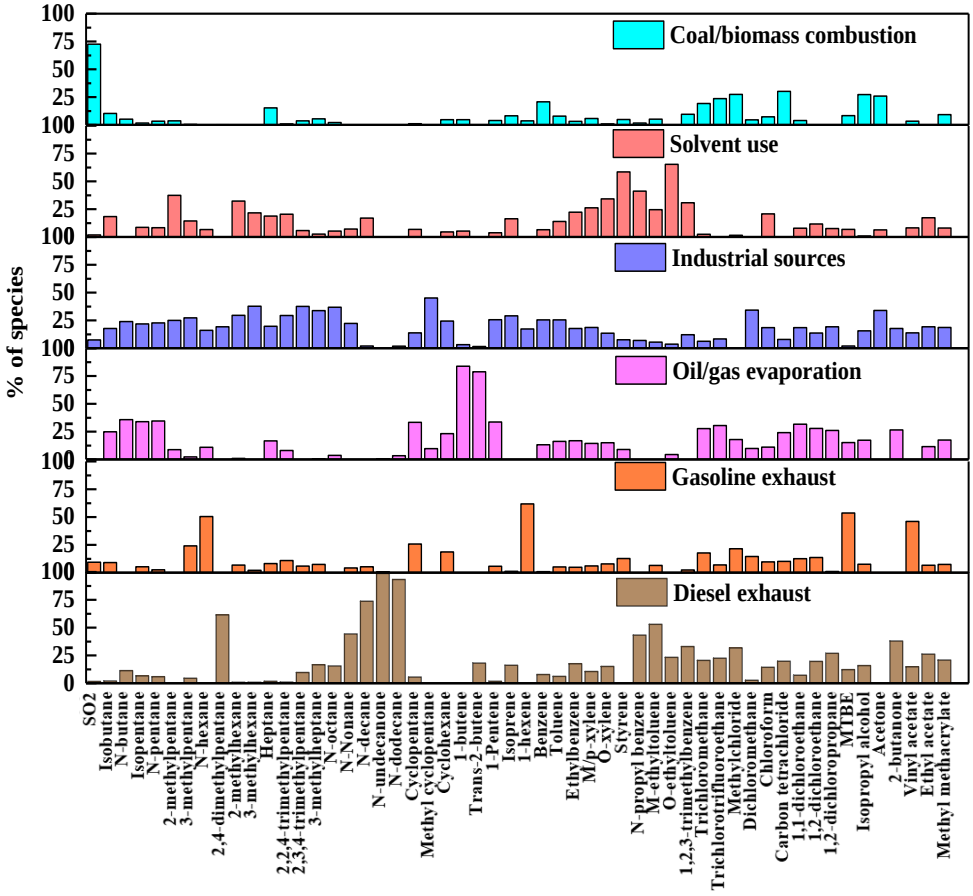

https://doi.org/10.5194/acp-2021-959
Preprint. Discussion started: 23 December 2021




**Fig. 7**

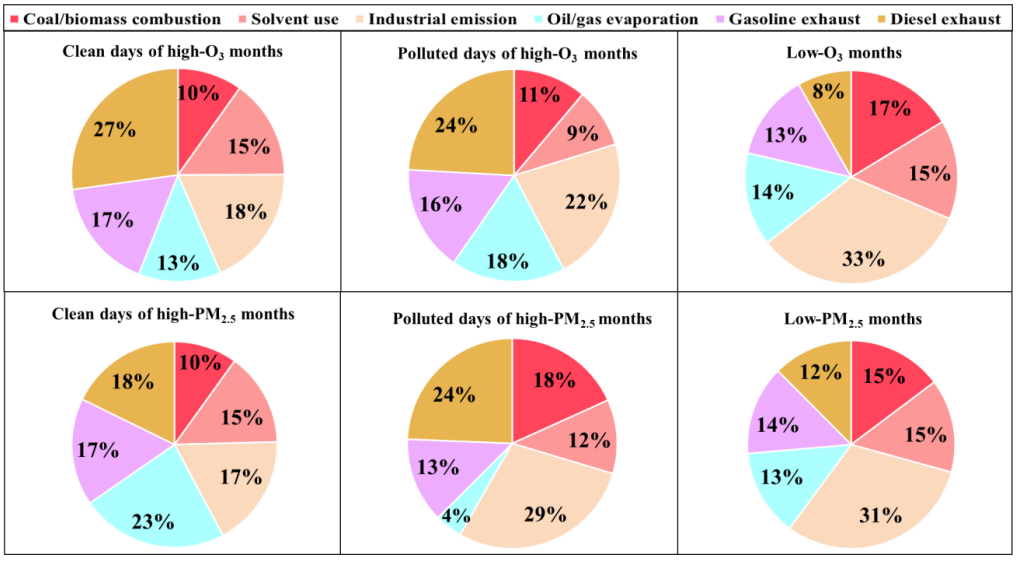

https://doi.org/10.5194/acp-2021-959
Preprint. Discussion started: 23 December 2021




**Fig. 8**

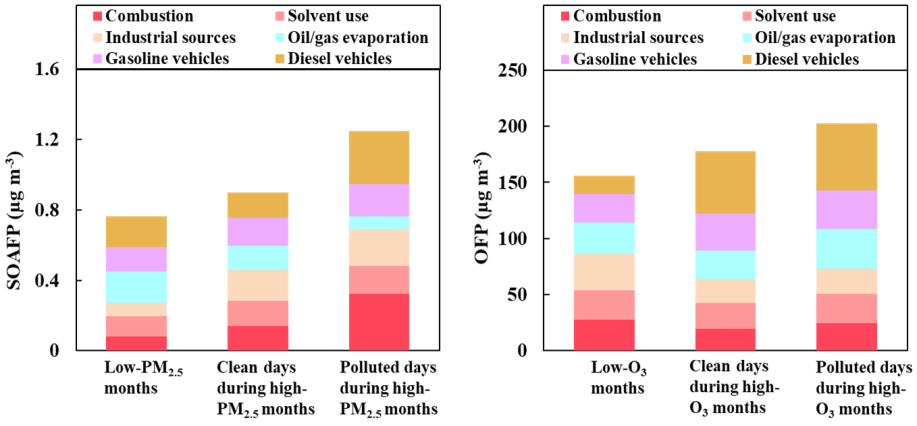

https://doi.org/10.5194/acp-2021-959
Preprint. Discussion started: 23 December 2021


Atmospheric Chemistry and Physics Discussions

**Fig. 9**

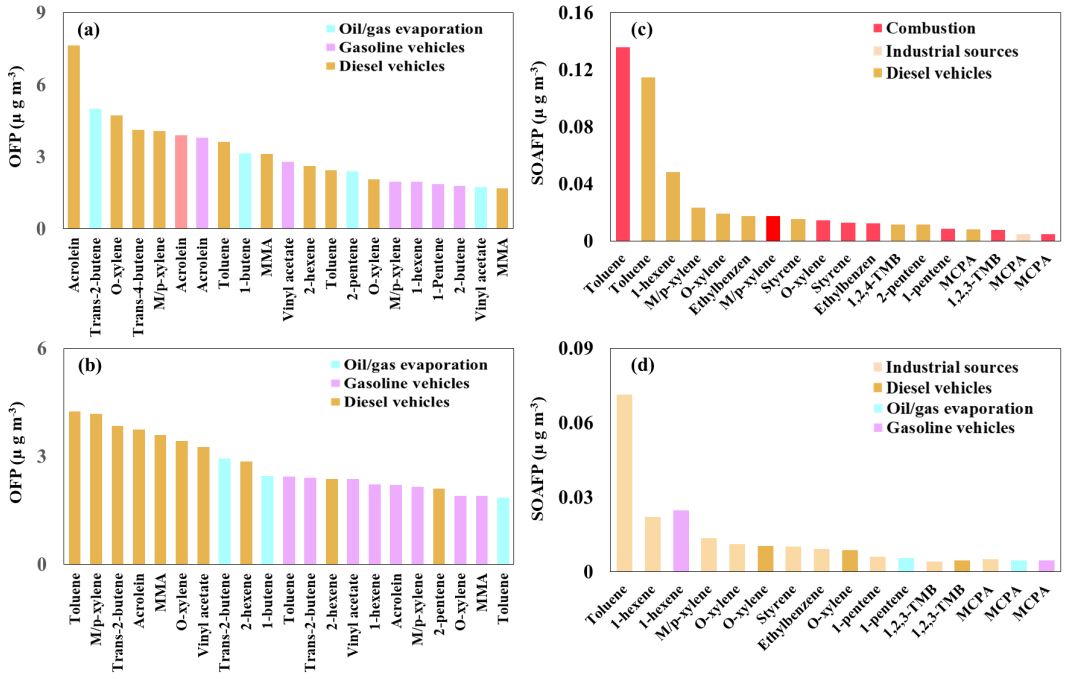

https://doi.org/10.5194/acp-2021-959
Preprint. Discussion started: 23 December 2021




**Fig. 10**

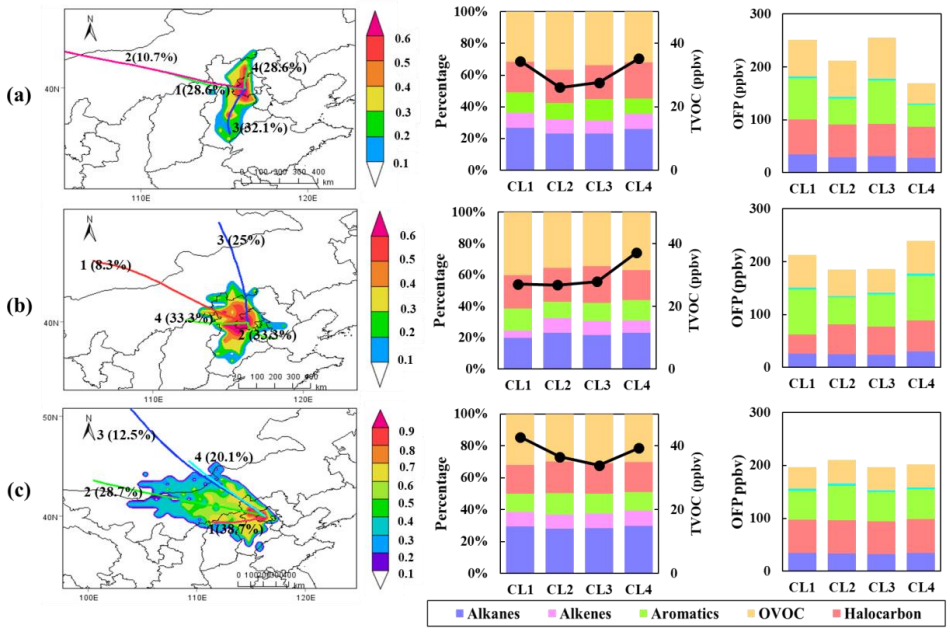

https://doi.org/10.5194/acp-2021-959
Preprint. Discussion started: 23 December 2021


Atmospheric Chemistry and Physics
Discussions

**Fig. 11**